

# Dependence of the electro-optical properties of polymer dispersed liquid crystals on the photopolymerization process

J. D. LeGrange,<sup>a)</sup> S. A. Carter,<sup>b)</sup> M. Fuentes,<sup>c)</sup> J. Boo, A. E. Freeny, W. Cleveland, and T. M. Miller<sup>d)</sup>

*Bell Laboratories, Lucent Technologies, 600 Mountain Avenue, Murray Hill, New Jersey 07974*

(Received 17 October 1996; accepted for publication 15 January 1997)

We have studied the dependence of the electro-optical properties of polymer dispersed liquid crystals (PDLC) on the ultraviolet (UV) cure of the solution of monomer and liquid crystal. The kinetics of UV polymerization and its effect on the morphology of the phase separated droplets of liquid crystal determine the switching voltage, response time, and luminance of the PDLC. Using a series of statistically designed experiments, we have mapped the dependence of these responses on the weight fraction of liquid crystal, the temperature of the cell during cure, and light intensity. Temperature and composition are strongly coupled parameters that influence switching voltage, luminance, and response times. Switching voltages are minimized at 4–5 V for an 8  $\mu\text{m}$  cell gap over a large region of temperature-composition space. An abrupt transition line occurs through that space. On one side of the transition line, voltage increases linearly either as temperature increases or composition decreases, and on the other side of the line, voltage is constant. Analyses of decay times, the slower response time of the PDLC, show that the times peak along a line of points in temperature-composition space that is close to the transition line for increasing switching voltages. We present these results as contours on the same graphs and relate them to our understanding of the phase separation process in the PDLC mixture. © 1997 American Institute of Physics. [S0021-8979(97)05408-X]

## I. INTRODUCTION

Portable products such as personal digital assistants and wireless communicators drive the need for lightweight displays that can be easily read in both artificial and natural lighting. Reflective displays that are visible in ambient lighting and operate without back lights reduce both the weight and power dissipation of a portable terminal. Polymer dispersed liquid crystals (PDLCs) are promising materials for reflective displays because they do not require polarizers and appear white in the unswitched state. This gives them the potential to be brighter than reflective twisted nematic (TN) or supertwisted nematic (STN) displays.<sup>1–3</sup>

PDLCs are made by inducing phase separation in a homogeneous mixture of liquid crystal and monomers by polymerizing the matrix either by thermal curing, UV curing, or by evaporation of a solvent. As the monomer polymerizes, the liquid crystal phase separates into droplets or domains separated by “walls” of the cured polymer matrix.<sup>4,5</sup> In the unaddressed state, the nematic texture within the domains is randomly oriented with respect to neighboring domains, and the display appears white due to light scattering. The addressed state, where the droplets align in the applied field, is transparent. Aligning the drops reduces both the scattering between neighboring drops and the scattering at the boundary between the polymer and the liquid crystal. The latter is true because the liquid crystal is chosen so that its ordinary index of refraction is matched to the index of the polymer.

Phase separation induced by uv polymerization is rapid and permits the tailoring of electro-optic properties through control of both the degree of polymerization at the time of phase separation and the rate of polymerization. Switching voltage, response times, brightness, and contrast of PDLC displays depend on the morphology of the liquid crystal droplets. The size and shape of these droplets depend on the composition, defined as the weight percentage of liquid crystal, and the temperature during the polymerization. The effect of temperature and composition can be understood by looking at the phase diagram for a PDLC mixture, as shown in Figure 1.<sup>5</sup> Phase separation occurs along the boundary in temperature-composition space between the isotropic region and the isotropic-nematic (I+N) two-phase region. At points below this boundary, the homogeneous mixture separates into a liquid crystal phase in a polymer matrix. Upon irradiation of the homogeneous mixture with UV light, polymerization begins and the average molecular weight increases. The phase separation boundary moves to higher temperatures. When the degree of polymerization is such that the temperature of cure corresponds to the temperature of phase separation for the composition of the mixture, liquid crystal droplets form.<sup>4,5</sup> If the PDLC composition and temperature during cure are far from the phase separation line, the matrix will be more polymerized at the onset of phase separation and the liquid crystal domains have less time to grow before the sample is solidified. Inspection of the phase diagram leads to the expectation that higher temperatures favor smaller liquid crystal domains. The viscosities of the polymer matrix and the liquid crystals, however, are lower at high temperatures, driving the formation of larger domains. In addition to the thermal effects on the size distribution of the liquid crystal dispersion, the droplet growth kinetics can

<sup>a)</sup>Electronic mail: jdl@lucent.com

<sup>b)</sup>Currently at Physics Dept., University of California, Santa Cruz, CA 95064.

<sup>c)</sup>Currently at Statistics Dept., University of Chicago, 5734 University Ave., Chicago, IL 60637.

<sup>d)</sup>Currently at CPS Chemical Co. Inc., Old Bridge, NJ 08857.

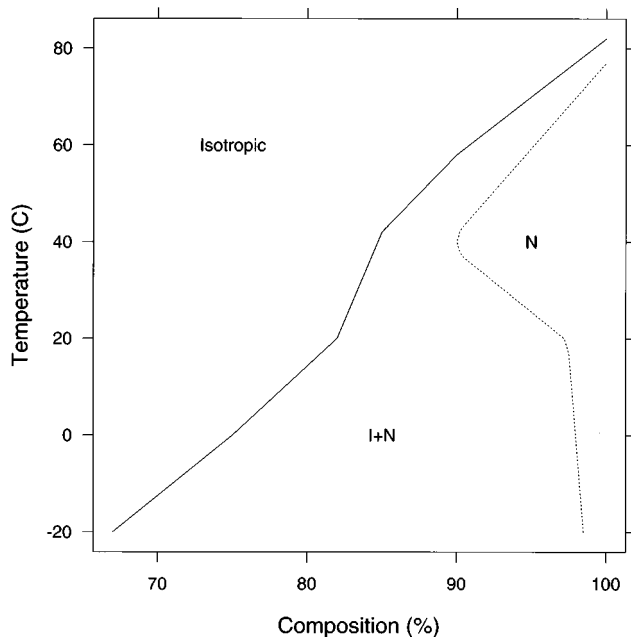


FIG. 1. Phase diagram (see Ref. 5) for PDLC mixture of liquid crystal and monomers for high liquid crystal composition with boundary at which phase separation occurs. At temperatures and compositions below the boundary, the homogeneous mixture of liquid crystal and monomers phase separate to form regions of nematic liquid crystal separated by monomer. Ultraviolet polymerization of the mixture leads to increase of the average molecular weight of the prepolymer components and a shift of the phase separation line to the northwest.

be affected by the intensity of the UV cure; a slow cure, for example, allows the droplets to grow to a larger size before the matrix is fully crosslinked.

We have used design of experiments methods to characterize the UV polymerization process and to understand the dependence of display drive voltages, response times, brightness, and contrast on composition, temperature, and light intensity. We chose to do statistically designed experiments because we need to know what process parameters to use in order to fabricate displays with specified properties. We had identified three relevant parameters with at least two of them strongly coupled. The use of design of experiments reduces the number of experiments that are needed to obtain a model describing the dependence of the measured responses on process parameters. In this paper, we describe these experiments and the statistical methods used to characterize the electro-optic responses.

## II. PDLC CELL ASSEMBLY

We fabricated single pixel PDLC test displays by making empty cells of uniform cell gap and then filling them with the PDLC mixture using capillary filling. The empty cells were assembled from large glass plates, 320 mm×400 mm, which had been coated with indium-tin-oxide (ITO) and photolithographically patterned. Plastic, spherical spacers of either 8  $\mu\text{m}$  or 10.5  $\mu\text{m}$  diameter were sprayed on one plate. We drew a glue pattern for 25 test cells on the opposing plate, using a computer controlled glue dispenser. The plates were then tacked together and placed in a plastic bag which

was heat sealed under vacuum. We used a uv curable glue which is cured by placing the vacuum bag under a uv lamp, followed by baking at 120 °C in order to ensure that the glue is completely crosslinked and does not react chemically with the PDLC components. The glue pattern consists of two beads along two opposite edges, and two dots on each of the top and bottom edges in order to leave gaps for capillary filling. After the glue was cured, we used a computer to scribe the plates prior to breaking them into 25 test cells. This procedure resulted in variation on the order of a few tenths of a micron in the gaps of the cells of a single plate-pair. All of the cells exhibited similar interference fringes showing that the cell gap variation was constant from cell to cell.

The PDLC mixture consists of an acrylate based monomer mixture (Merck PN393) and a superfluorinated liquid crystal mixture (Merck TL213). The liquid crystals, which make up roughly 80% of the PDLC mixture by weight, contain fluorinated and chlorinated aromatic groups, and exhibit a high birefringence between 0.2 and 0.3, which leads to enhanced light scattering. We varied the weight percentage of the liquid crystal from 76% to 82%.

We filled the cells by tilting them on a shim and pipetting several drops of the mixture at one of the open edges of the cell. The filled cells were then cured by broad band uv light with an emission maximum at 365 using an infrared filtered, uniform light source. In experiments where we studied the effect of light intensity on electro-optic properties, we varied light intensity from 22  $\mu\text{W}/\text{cm}^2$  to 16  $\text{mW}/\text{cm}^2$ . In the range 8–16  $\text{mW}/\text{cm}^2$ , the time of irradiation was varied so that the total energy was 6.4  $\text{J}/\text{cm}^2$ . For intensity below 8  $\text{mW}/\text{cm}^2$ , we irradiated for 5 min during which the final morphology is established; this was followed by additional irradiation at 16  $\text{mW}/\text{cm}^2$  for 400 s in order to ensure that the total energy was constant and that the polymer matrix was completely cross-linked. Before exposing the cells to UV radiation, we equilibrated them on a temperature controlled platen for which we varied the temperature from 6 °C to 38 °C.

## III. DESIGN OF EXPERIMENTS

Fabrication of displays for product prototypes requires knowledge of the switching voltage, response times, and optical properties of the display. In order to elucidate the dependence of these properties on composition, intensity of the uv light (defined as cure in all plots), and temperature of the PDLC during cure, we began by running a full factorial experiment in which two levels were selected for each parameter.<sup>6</sup> Samples were made for all combinations of the different levels for the parameters giving a total of  $2^3=8$  samples. In addition, we made a ninth sample using the midpoint of each parameter. We ran the experiment twice at these nine combinations of the parameters and three times at the combination at the high level of each parameter. It is difficult to obtain the exact nominal values for some of the process factors as composition which is expressed as weight percent of liquid crystal, therefore the actual readings are not exactly at the nominal levels of the parameters. After running this design and obtaining reproducible results, we ran a

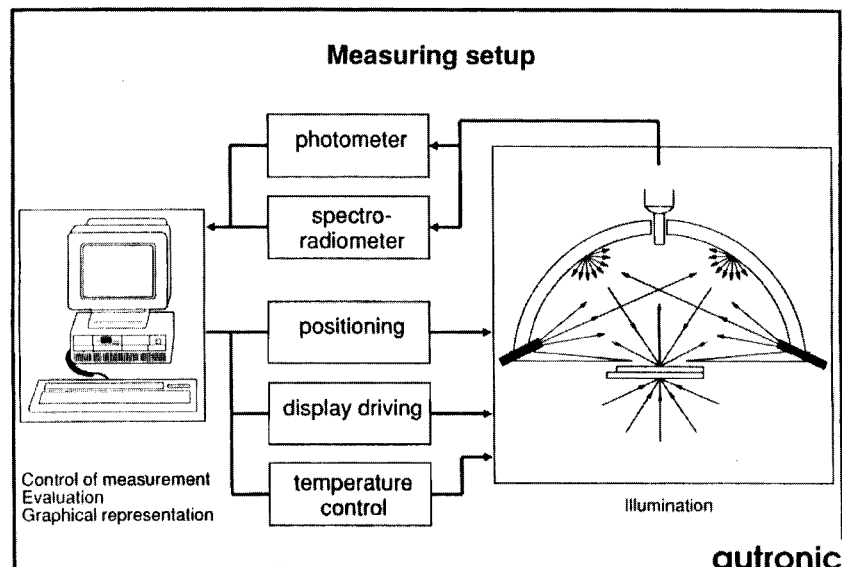


FIG. 2. Schematic of the apparatus used to measure display reflectivity as a function of voltage. White light from a diffusing hemisphere is incident on the sample. The reflected light is collected through a slit in the hemisphere and measured by a photomultiplier tube.

series of simpler designs covering a smaller range of parameters to study only one or two of the parameters while holding the remaining ones fixed.

#### IV. ELECTRO-OPTIC MEASUREMENTS

We measured reflectivity for all of the above samples as a function of voltage at normal viewing angle using a display measurement system (Autronic-Melchers DMS-703) equipped with a diffuse, depolarized white light source.<sup>7</sup> The PDLC test cell was placed on top of velvetized paper which we used as the black absorber. The measurements were done in a reflective mode with light from a 150 W cold-light source incident on the sample from a diffusing hemisphere, shown schematically in Figure 2. The reflected light from a 3 mm diameter spot on the display passes through a slit in the hemisphere, and then is coupled by a microscope objective into a fiber bundle leading to a detector. The detector is a photomultiplier tube adjusted to the spectral sensitivity of the human eye. We measured reflectivity as a function of voltage from 0 to 20 V. We recorded switching voltage as  $V_{90}$ , the voltage for which the reflectivity is 90% of the maximum change. We used 30 V for samples that were 90% switched at voltages greater than 14 V, since those samples were not completely switched at 20 V. We measured on and off response times using either 10 or 20 V to switch the cell; 20 V was used for cells with  $V_{90}$  greater than 14 V. Initially, we calculated contrast as the ratio of reflectivity in the scattering state to that of the switched state; however, we could not fit a model to the data due to the large variability in both the numerator and denominator. Alternatively, we decided to measure absolute luminance in the white state in order to reduce the variability due to variations in ambient lighting, incident light source, and in the reflectivity of the top glass plate. We normalized the reflectivity of the scattering state to

that of a 42% brightness standard, and then used the ratio of the reflectivity in the white and black states to derive the standardized luminance of the black state.

#### V. STATISTICAL ANALYSIS OF RESULTS

The process parameters and measured responses for the samples made for seven experiments are tabulated in Table I. The first 19 samples (experiments 1 and 2) are the following: (1) two replications for all combinations of the parameters with nominal levels of 78% and 82% for composition, 24 °C and 38 °C for temperature, and 8 mW/cm<sup>2</sup> and 16 mW/cm<sup>2</sup> for light intensity; (2) a third replication for the combination at the high level of each parameter; (3) two replicates for the mid-point sample of 80% liquid crystal, 12 mW/cm<sup>2</sup> cure, and 31 °C temperature. Due to the difficulty in obtaining the exact nominal levels for some of the process factors, the actual readings are not exactly at the nominal values. In analyzing the results from these samples, we first studied the dependence of switching voltage on the process variables.

Figure 3 shows a scatter plot for composition and temperature space for the 43 samples of experiments 1–5, the samples with the 8 μm spacers. The diagonal line is a transition line whose equation will be given below. For samples fabricated at conditions to the right of this line, voltage does not depend on temperature or composition; in this region, the voltages vary around a value of about 5 V, for an 8 μm cell gap. For samples made at conditions to the left of the line, voltage is a linear function of temperature and composition, and increases as either composition decreases or temperature increases.

To account for this observed behavior of the data, we fit a model that is a piecewise-linear, continuous spline in composition and temperature; the spline consists of two planes that join at the transition line. On one side of the transition line, voltage is linear in temperature and composition, and on

TABLE I. Data.

Expt No.	Spacer ( $\mu\text{m}$ )	Comp (%)	Temp ( $^{\circ}\text{C}$ )	Intensity ( $\text{mW}/\text{cm}^2$ )	$V_{90}$ V	$T_{\text{on}}$ (msec)	$T_{\text{off}}$ (msec)	Luminance (%)
1.0	8.0	81.9	24.0	8.5	5.7	22.0	122.0	
1.0	8.0	81.9	24.0	16.3	5.9	22.5	121.4	
1.0	8.0	81.9	38.0	16.3	6.0	26.8	140.7	
1.0	8.0	81.9	38.0	16.3	5.7	27.4	140.4	
1.0	8.0	81.9	38.0	8.5	7.3	31.9	94.2	
1.0	8.0	78.0	38.0	16.1	18.9	11.9	8.0	
1.0	8.0	78.0	38.0	8.5	19.0	10.8	7.6	
1.0	8.0	78.0	24.0	16.1	7.5	34.5	85.7	
1.0	8.0	78.0	24.0	8.5	9.4	41.0	78.4	
1.0	8.0	79.8	31.0	12.5	7.0	26.7	126.4	
2.0	8.0	78.2	24.0	8.5	7.4	26.6	108.2	26.7
2.0	8.0	78.2	24.0	16.0	5.9	23.4	170.6	27.7
2.0	8.0	78.2	38.0	16.0	18.5	17.6	11.4	28.7
2.0	8.0	78.2	38.0	8.0	18.8	11.4	9.6	29.8
2.0	8.0	81.9	38.0	16.0	4.8	21.2	152.4	24.0
2.0	8.0	81.9	38.0	8.0	6.1	26.6	112.6	25.4
2.0	8.0	81.9	24.0	8.0	6.2	22.6	73.2	20.6
2.0	8.0	81.9	24.0	16.0	5.6	20.4	116.2	22.7
2.0	8.0	80.2	31.0	12.0	6.3	24.2	176.6	28.2
3.0	8.0	77.5	24.0	16.0	12.0	59.2	49.6	26.3
3.0	8.0	77.5	32.0	16.0	19.0	13.5	11.4	27.7
3.0	8.0	77.5	28.0	16.0	15.9	39.5	22.3	26.3
3.0	8.0	77.5	36.0	16.0	22.8	9.8	12.1	27.4
3.0	8.0	79.1	36.0	16.0	17.2	14.1	21.1	24.2
3.0	8.0	79.1	24.0	16.0	4.9	23.1	295.0	24.6
3.0	8.0	79.1	28.0	16.0	7.2	31.7	138.0	26.8
3.0	8.0	80.4	24.0	16.0	5.0	23.0	213.0	21.7
3.0	8.0	80.4	36.0	16.0	10.7	52.4	56.4	23.9
3.0	8.0	80.4	32.0	16.0	5.8	26.9	190.0	25.0
3.0	8.0	80.4	28.0	16.0	4.7	26.3	337.0	22.9
3.0	8.0	80.4	36.0	16.0	5.0	46.6	59.6	23.9
4.0	8.0	78.9	24.0	16.0	4.7	21.2	315.0	23.2
4.0	8.0	78.9	28.0	16.0	7.5	24.2	94.4	29.2
4.0	8.0	78.9	32.0	16.0	4.7	38.6	38.6	26.5
4.0	8.0	80.0	24.0	16.0	4.7	21.5	238.0	23.2
4.0	8.0	80.0	28.0	16.0	4.5	21.7	306.0	24.7
4.0	8.0	80.0	32.0	16.0	7.6	28.8	97.5	28.0
4.0	8.0	78.9	24.0	16.0	4.8	21.3	239.0	20.9
4.0	8.0	78.9	24.0	16.0	4.7	18.1	199.5	23.1
5.0	8.0	76.0	24.0	16.0	19.6	14.6	17.2	28.7
5.0	8.0	76.0	20.0	16.0	10.6	44.2	57.1	29.8
5.0	8.0	76.0	16.0	16.0	8.6	59.7	122.6	27.9
5.0	8.0	76.0	12.0	16.0	7.2	28.7	96.6	24.5
6.0	10.5	78.2	20.0	16.0	7.9	75.0	129.4	33.1
6.0	10.5	78.2	15.0	16.0	8.7	52.9	91.8	32.7
6.0	10.5	78.2	15.0	16.0	7.1	38.2	145.4	29.4
6.0	10.5	78.2	10.0	16.0	7.6	43.2	138.5	30.3
6.0	10.5	78.2	10.0	16.0	shorted			25.9
7.0	10.5	78.1	20.0	6.0	7.3	45.7	170.5	33.0
7.0	10.5	78.1	20.0	0.0	8.2	48.7	114.0	24.0
7.0	10.5	78.1	20.0	8.0	10.2	94.7	299.0	39.0
7.0	10.5	78.1	20.0	16.0	7.7	48.4	149.1	33.0
7.0	10.5	78.1	28.0	16.0	17.0	16.5	39.2	35.0
7.0	10.5	78.1	20.0	0.2	8.0	51.7	140.4	25.0
7.0	10.5	78.1	28.0	0.2	23.6	35.8	24.2	31.0
7.0	10.5	78.1	20.0	2.1	7.1	39.9	153.6	30.0
7.0	10.5	78.1	28.0	2.1	21.8	27.7	26.7	30.0
7.0	10.5	78.1	28.0	8.0	20.1	24.9	31.3	33.0
7.0	10.5	79.9	20.0	2.1	7.2	44.7	186.5	25.0
7.0	10.5	79.9	20.0	0.2	7.7	48.7	171.2	25.0
7.0	10.5	79.9	20.0	6.0	6.7	38.4	174.8	28.0
7.0	10.5	79.9	20.0	16.0	7.0	38.7	152.4	30.0
7.0	10.5	79.9	20.0	0.0	8.1	57.5	166.3	24.0
7.0	10.5	79.9	20.0	8.0	6.7	37.1	172.4	30.0

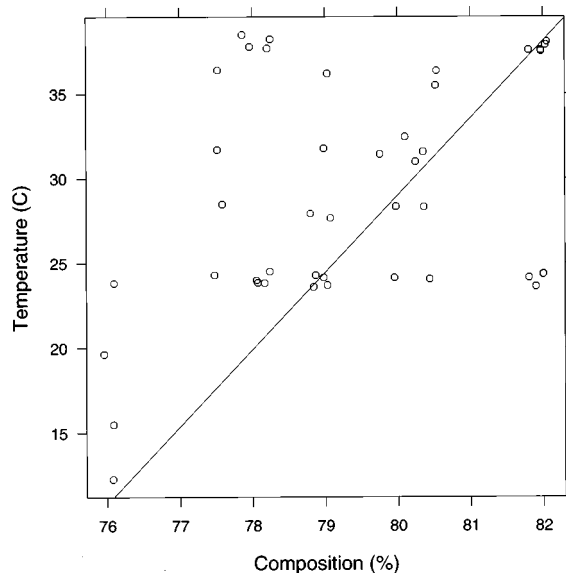


FIG. 3. A scatter plot showing the coordinates in the temperature and composition space for experiments 1–5. A small amount of uniform random noise has been added to the plotting locations to prevent plotting symbols from being obscured. The line is the fitted transition line from the spline model relating switching voltage to temperature and composition.

the other side of the line, voltage is constant, just as we observed in the data. We fitted this model by least squares. The estimated transition line which has been displayed in Figure 3 is

$$C = 73.62 + 0.22T,$$

where  $C$  is composition expressed as weight percent of liquid crystal and  $T$  is temperature in °C. The estimated model is

$$V = -3.9[C - 73.62 - 0.22T]^+ + 5.1,$$

where  $V$  is voltage in volts and the notation  $[x]^+$  means  $x = x$  if  $x > 0$  and is zero otherwise. All coefficients are highly statistically significant.

The slope of 0.22 of the transition line is roughly the same as the slope of the curve between the isotropic and isotropic/nematic phases in the phase diagram of Figure 1. Thus points along lines parallel to the transition line are equidistant from the phase separation line, and therefore have the same switching voltage.

We will now present both the data and the model. Switching voltage as a function of temperature for a given composition is displayed for the first five experiments in Figure 4 by a Trellis plot.<sup>8</sup> The plotting symbols on each panel of the figure are a scatterplot of switching voltage against temperature for values of composition in an interval. The seven intervals are 76.00%–76.00%, 77.52%–77.52%, 77.96%–78.24%, 78.90%–79.08%, 79.82%–80.16%, 80.43%–80.43%, and 81.90%–81.94%. The intervals, which are portrayed by the darkened bars in the top strip, are ordered from low to high as we go from left to right and then from bottom to top through the panels; they cover the range of values of composition in the experiments. The switching voltages of samples cured at light intensities other than 16

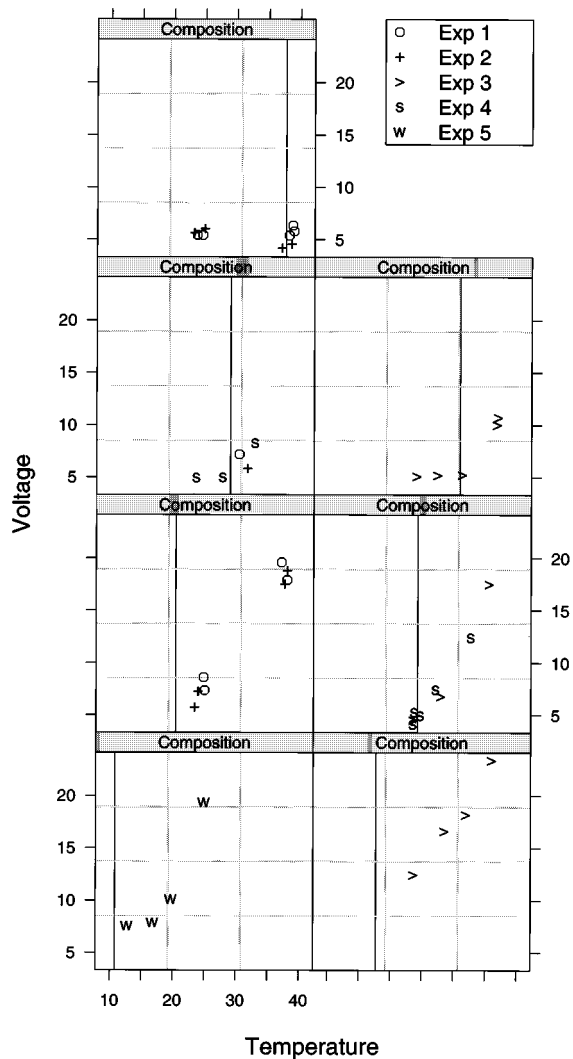


FIG. 4. A Trellis plot of switching voltage as a function of temperature for given intervals of composition. The data are from experiments 1–5. A small amount of uniform random noise has been added to the plotting locations to prevent plotting symbols from being obscured. These plots show that for each value of composition, there is a threshold value of temperature above which the switching voltage increases and below which it is constant. The vertical line on each panel is at the threshold temperature of the observations on that panel. Light intensity is fixed at 16 mW/cm<sup>2</sup> in experiments 3–5. The voltages for samples from experiments 1 and 2 cured at lower light intensities were adjusted for intensity. Some noise has been added to temperature values in the righthand panel in the second row to avoid overlapping symbols.

mW/cm<sup>2</sup> were corrected by subtracting 16 mW/cm<sup>2</sup> from light intensity and then multiplying the difference by the estimated coefficient for light intensity from a model fit to the voltages measured in experiments 1 and 2.

The Trellis display shows clearly the structure of the data. For a given composition, the voltage is approximately constant with temperature until a threshold temperature is reached, and then the voltage increases linearly. The vertical line on each panel shows the threshold; it is computed from the fitted transition line of the model.

Figure 5 shows the data and the model in a different way. Voltage is plotted against an axis in composition-temperature space that is perpendicular to the transition line. The vertical line marks where this axis equals 0 and repre-

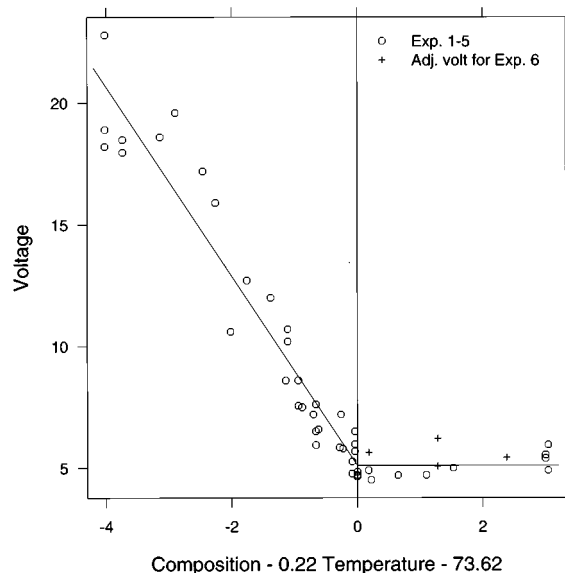


FIG. 5. A 2-dimensional representation of the voltage data from experiments 1–5 as a function of the composite variable defined by the formula labelling the abscissa. The vertical line defines the 0 value for this composite variable where the transition between constant and linearly increasing voltage occurs. The slope of the left line and constant value of the right line were determined by least squares fitting to the appropriate points. The crosses, which are points from experiment 6, represent values of voltage that have been scaled to account for the larger cell gap, and agree well with the fitted line.

sents the threshold for the transition from constant to changing voltage. The crosses in Figure 5 are points from the sixth experiment where the cells were made with  $10.5 \mu\text{m}$  spacers instead of  $8 \mu\text{m}$  spacers; the voltages were scaled by dividing by the ratio of the two gaps. We verified that this adjustment is supported by the data; we fit a model for voltage as a function of composition and temperature that contained a multiplicative constant for the voltages for the  $10.5 \mu\text{m}$  spacers, and the resulting fit yielded voltages within 5% of those that we got from our ratio adjustment.

We fit a model to response time as a function of composition and temperature. We used the switching from the clear to scattering state because this is generally the slower response time. We used the 34 samples from experiments 1–5 for which the switching voltage is less than 14 V. The response time was treated in a way similar to our treatment of voltage; that is, we fit a model in which response time as a function of temperature and composition consists of two planes that join at a transition line; but in this case neither plane has zero slope. The estimated transition line is

$$C = 72.11 + 0.29T.$$

The estimated model is

$$R = -140.6 - 52.08[C - 72.11 - 0.29T]^+ + 107.63[C - 72.11 - 0.29T]^-,$$

where  $R$  is the response time in milliseconds, and the notation  $[x]^-$  means  $x = x$  if  $x < 0$  and is zero otherwise. All coefficients are highly statistically significant. Figure 6

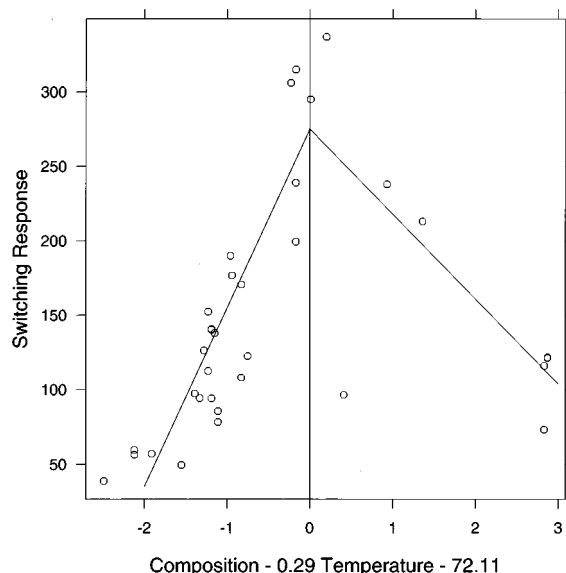


FIG. 6. This plot of the dependence of response time on composition and temperature is carried out in the same way as Figure 5. The response time as a function of the composite variable is described by a line of increasing slope that reaches a peak value and then decreases for increasing values of the composite variable. The vertical line marks where the composite variable equals 0 and the response time peaks.

graphs the data and the model in the same manner as Figure 5.

We also fit standardized luminance data for experiments 2–6. Figure 7 is a Trellis plot of the standardized luminance as a function of temperature for different levels of composition. There is a peak in standardized luminance as a function of temperature. Such a peak may correspond to a peak in backscattering due to the optimum drop size for light scattering.<sup>9</sup> Furthermore, brightness tends to increase with decreasing composition. In order to account for the nonlinearity in the dependence of luminance on temperature, we fit a model to the data, which is linear in cure intensity and composition, and quadratic in temperature. The estimated model is

$$L = 123.53 + 0.56T - 0.007T^2 - 1.34C - 0.2I,$$

where  $I$  is the cure intensity in  $\text{mW}/\text{cm}^2$  and  $L$  is the luminance expressed as brightness percent. All coefficients are highly statistically significant.

## VI. RESULTS: SUMMARY AND DISCUSSION

The three responses — standardized luminance, switching voltage, and response time — can be viewed with contour plots which are based on the models derived from the data. Figure 8 displays contours for standardized luminance plotted in composition-temperature space for three different light intensities. The line dividing the constant low voltage regime characterized by switching voltages of 5.1 V is shown by the dashed line. Points below and to the right of this line define a plane of increasing voltage. A second dashed line, parallel to the 5.1 V break line, shows the line of points that gives switching voltages of 7 V.

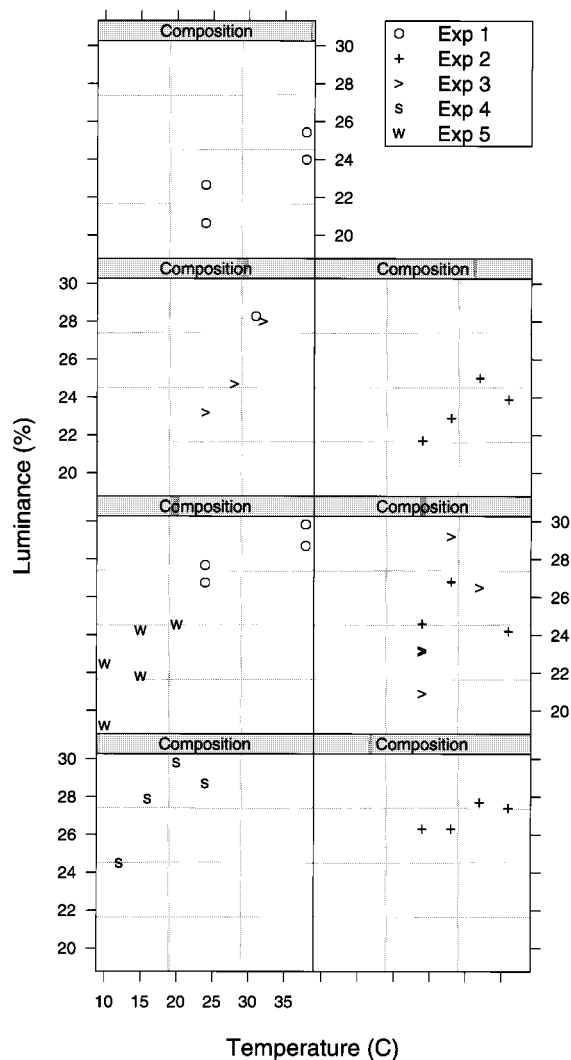


FIG. 7. A Trellis plot of standardized luminance against temperature for different levels of composition. The data, which are from experiments 2–6, suggest that there is a peak in luminance at a critical temperature and that the peak shifts to a higher temperature for a higher composition.

Previous results suggest that as the liquid crystal droplets grow in size, the switching voltage decreases and the off time increases.<sup>1,4,5</sup> The voltage at which the PDLC exhibits 90% of its maximum transmission ( $V_{90}$ ) depends on droplet size  $R$ , droplet anisotropy  $L$ , cell gap  $d$ , and the elastic constants  $K$  and the dielectric anisotropy  $\Delta\epsilon$  of the liquid crystal according to the following expression:<sup>1,3,10</sup>

$$V_{90} \propto d/R(L^2 - 1)^{1/2} (4\pi K/\Delta\epsilon)^{1/2}.$$

$L = R_2/R_1$ , where  $R_2$  and  $R_1$  are the major and minor radii of an elliptical drop. The interaction of the electric field with the liquid crystal competes with the interfacial energy between the liquid crystal and the polymer wall of the droplet. Smaller droplets are harder to switch because of larger anchoring energies. Both the dielectric anisotropy and anchoring energy are affected by the configuration of the liquid crystal director. The off-time  $\tau_{\text{off}}$  is proportional to the rotational viscosity of the liquid crystal  $\gamma$ , and depends on droplet size, droplet anisotropy, and the liquid crystal elastic constant according to the expression

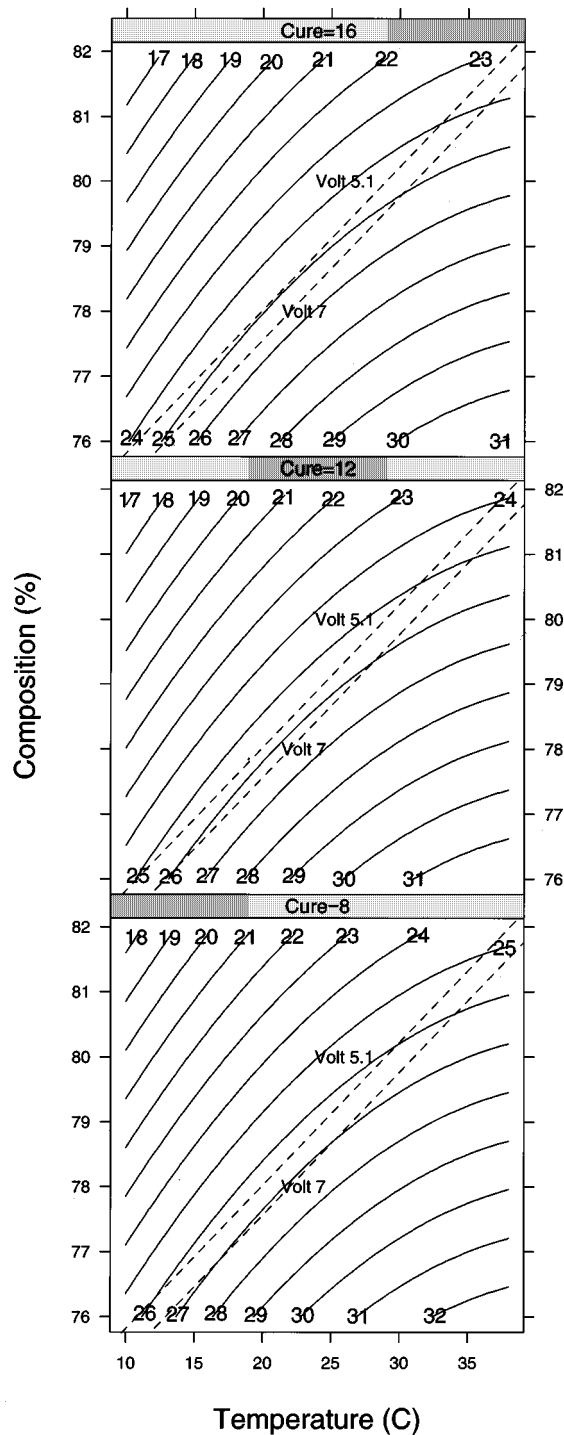


FIG. 8. A Trellis plot displaying contours of luminance as a function of composition and temperature for different light intensity levels. The lines superimposed on the plots mark the isovoltage lines for 5.1 V and 7 V.

$$\tau_{\text{off}} \propto \gamma R^2 / [K(L^2 - 1)].$$

This expression predicts that the off time is longer for larger drop size, therefore, as the switching voltage increases, the response time decreases.<sup>1,3,10</sup>

Our results for response time and switching voltage show that this simple model based on drop size and shape does not describe the electro-optic behavior of a PDLC. Response time does not correlate with switching voltage. We

have shown that the switching voltage increases after a threshold value of composition and temperature. Below the composition-temperature line at which the transition occurs between constant voltage and linearly increasing voltage, the response time increases even though switching voltage is constant. In the region where voltage increases linearly, the data are consistent with the above equations since response time decreases with increasing voltage. PDLCs exhibit increasing drop size as a function of composition in the range of 76–82 wt %. The drops remain circular over this range.<sup>5</sup> The fact that switching voltage is constant over a large area of temperature-composition space does not agree with the idea that voltage scales with drop size. We have shown that the same switching voltage may be obtained over a large range of drop sizes. This suggests that the anchoring energies are small and that the electro-optic behavior in the region of constant voltage is determined mainly by the dielectric anisotropy.

We have also studied the dependence of switching voltage and standardized luminance on light intensity in the range of  $22 \mu\text{W}/\text{cm}^2$ – $16 \text{mW}/\text{cm}^2$  with the idea that a very slow cure would lead to larger drops and therefore low switching voltages. We found that at 78% and 80% composition and at 20 °C, conditions on the constant voltage side of the transition line, voltage is constant with light intensity. On the other hand, at 78% composition and 28 °C, which is in the linear increasing regime, there is a slight decrease in voltage as intensity increases, a result that is in fact opposite to what we expected since higher intensity implies a faster cure of the polymer and, therefore, less time to grow large droplets. Luminance as a function of light intensity for the same samples, reaches a maximum value at about  $8 \text{mW}/\text{cm}^2$ . This is consistent with a peak in the backscattering at some optimum drop size.<sup>9</sup>

## VII. CONCLUSIONS

We have mapped out the dependence of standardized luminance, switching voltage, and response time on the liquid crystal weight fraction, on temperature during cure, and on light intensity by using a series of statistically designed experiments and by fitting models to the resulting data. The standardized luminance behaves as we would expect from our knowledge of the light scattering properties of PDLCs, confirming that the light scattering behavior is dominated by

liquid crystal droplet size and shape. The switching voltage and response time behavior, however, cannot be explained by a simple model based on drop size. The transition from constant, low voltages to a linearly increasing function suggests a sudden change in morphology, either in the domain shape or in the liquid crystal director configuration. One possible explanation is that the anchoring energy is small and that electric field effects dominate over the region on the low composition and low temperature side of the break-line. We are currently extending the previous investigations based on confocal microscopy<sup>5</sup> in order to explain the electro-optic behavior of these PDLC materials.

PDLC materials based on photopolymerizable monomers have the advantage that the electro-optical properties may be controlled over a large range of values by varying liquid crystal weight fraction and both the cure temperature and light intensity. We have demonstrated by statistical methods that it is possible to make displays with reproducible properties over a large range of conditions. This reproducibility and the possibility for tuning the display properties make PDLC materials promising candidates for the manufacture of reflective displays for portable products.

## ACKNOWLEDGMENTS

The authors would like to thank Karl Amundson for his insights and many helpful discussions, Paul Mulgrew and Mike Anzlowar for fabrication of patterned ITO glass plates, and Eric Fefferman and Gary Dabbagh for scribing the glass and occasional assistance in cell assembly.

<sup>1</sup>J. W. Doane, *Mater. Res. Bull.* **16**, 22 (1991)

<sup>2</sup>J. W. Doane, N. A. Vaz, B.-G. Wu, and S. Zumer, *Appl. Phys. Lett.* **48**, 269 (1986).

<sup>3</sup>D. Coates, *Displays* **14**, 94 (1993).

<sup>4</sup>Y. Hirai, S. Niiyama, H. Kumai, and T. Gunjima, *Rep. of the Research Lab., Asahi Glass Co., Ltd.* **40**, 285 (1990).

<sup>5</sup>K. R. Amundson, A. van Blaaderen, and P. Wiltzius, *Phys. Rev. E* **55**, 1646 (1997).

<sup>6</sup>G. Box, W. Hunter, and J. Stuart Hunter, *Statistics for Experimenters* (Wiley, New York, 1978).

<sup>7</sup>M. E. Becker and J. Neumeier, *SID Dig.*, 163 (1990).

<sup>8</sup>R. A. Becker, W. S. Cleveland, and M. J. Shyu, *J. Comput. Graph. Stat.* **5**, 123 (1996); or for additional information, see <http://cm.bell-labs.com/stat/project/trellis/>.

<sup>9</sup>P. Wiltzius (unpublished data).

<sup>10</sup>B. G. Wu, Y. D. Ma, T. S. Li, and R. B. Timmons, *SID Dig.*, 583 (1992).